Design and Optimization of He-Xe Brayton cycles system for MW-level space nuclear reactor application*

Yun-Cheng Gao,[1,2] Si-Miao Tang,[1,2,†] Lu-Teng Zhang,[1,2] and Liang-Ming Pan[1,2]

[1] *Key Laboratory of Low-grade Energy Utilization Technologies and Systems, Ministry of Education, Chongqing University, Chongqing 400044, China.*

[2] *Department of Nuclear Engineering and Technology, Chongqing University, Chongqing 400044, China.*

Space reactor power has a good future in sea, land, air and space by virtue of its small size, applicability and high efficiency, and the combination of high temperature gas-cooled reactor and Brayton cycle is more suitable for exploration missions at the megawatt power level. A space gas-cooled reactor with a thermal power of 3 MW is used as a research object, and the design and optimization of this research object is carried out using EBSILON simulation software. The efficiency comparison between direct and indirect Brayton cycle is carried out under different conditions, the direct Brayton cycle was found to be 1.4%-2.8% more efficient than the indirect Brayton cycle and occupies less space. The efficiencies of four configurations of the Brayton cycle are compared. When the compressor inlet temperature is 400 K, the recompression efficiency is lower, and the efficiency of both the interstage-cooled cycle and the simple reheat cycle is higher than 30% when the turbine inlet temperature reaches 1400K. When the compressor inlet temperature is 350K, the simple reheat cycle can achieve 29.6% efficiency at a turbine inlet temperature of 1200K. When the compressor inlet temperature is 300K, the efficiency of all four cycle structures is higher than 20%. And when the turbine inlet temperature is higher than 1150K, the efficiency of all four structures is higher than 30%. The optimal pressure ratios are different for the different configurations, with 2.2 and 3.5 for the simple reheat cycle and the interstage-cooled cycle, respectively. And the optimal pressure ratio for the recompression cycle is also related to its diversion ratio, the recompression cycle efficiencies are 0.417 and 0.141 when the splitting ratios are 0 and 0.4, respectively. In actual operation, the pressure loss of the system is unavoidable. It is found that the efficiency reduction caused by the high pressure relative loss is 1.7% higher than the reduction caused by the low pressure relative loss. In addition, the recuperator effectiveness and the efficiency of the TAC also affect the system cycle efficiency to some extent. The exergy analysis method was also used to verify that the recompression cycle efficiency was lower than the simple reheat cycle efficiency. The losses in both are concentrated in the cooler and reactor, with the cooler and reactor losses of the recompression cycle together accounting for 79.6% of the total losses. Finally, the simple reheat cycle was taken as the optimal structure, and a space reactor system with a thermal power of 3 MW and an electrical power of 1 MW is successfully designed.

Keywords: Brayton cycle; Space nuclear reactor; Exergy analysis method; Design and optimization

I. INTRODUCTION

Energy is indispensable to industry, military and people's livelihood. And with the advancement of science and technology, mankind is now gradually strengthening its exploration of the sea, land, air and sky. However, solar energy is not an autonomous energy source, the mission cycle of chemical energy is short, and the power level of radioisotope nuclear power source is low. So for high-power level mission, the above energy sources can hardly be used[1] . The new mobile reactor system does not depend on sunlight and has high energy density, which has been widely studied and applied in the field of sea, land, air and space[2]. For the main technical of the space reactor system, it is necessary to consider three aspects: firstly, the safety and economy of the reactor power supply. Secondly, the performance of the reactor power supply, which is aim to improve the power to mass ratio of the reactor power supply as much as possible. And lastly, the applicability of the reactor power supply.

Based on the excellent characteristics of the new portable reactor system, as early as a few decades ago, some scholars in the world have done a lot of research on the space reactor power supply. In 2003, the United States NASA(National Aeronautics and Space Administration) set up a project "Prometheus" program, the main goal is to develop a high-power space nuclear reactor power supply[3]. In 2009, Russia began to develop the MWe-class nuclear propulsion spacecraft[4], which consists of an ultrahigh-temperature gas-cooled reactor and a Brayton cycle system, and it guides for the design and development of subsequent space reactors. ESA(European Space Agency) is also working on the "Prometheus" program. ESA is also vigorously developing space nuclear power technology, mainly through the implementation of the DiPoP(Disruptive Technologies for Power and Propulsion)[5] project and the MEGAHIT[6] program, and has completed the technical selection of various systems of nuclear electric propulsion.

Based on the exploratory experience of the previous researchers, more and more researches on the space reactors have appeared. Ju et al.[7] proposed a conceptual design scheme for a helium-xenon gas-cooled fast reactor consisting of hexagonal prismatic fuel elements, and also investigated the thermo-hydraulic characteristics of the reactor. Yang et al.[8] also presented the neutron physical analysis on a pris-

* This work is Funded by Natural Science Foundation of Chongqing, China2023NSCQ-BHX0243.

† Corresponding author, Si-Miao Tang, complete address:simiao_tang@cqu.edu.cn, telephone number:+86 18829581798.

matic space gas-cooled reactor. Jiang et al.[9] developed a simple mass estimation model based on a preliminary optimized shielding design for the Jupiter Icy Moon Orbiter (JIMO) reactor. Yue et al.[10]studied OMEGA (Open-grid Megawatt Gas-cooled spAce nuclear reactor) and also developed TASS (Transient Analysis code of scheduled Shutdown and emergency Shutdown). Based on this, it was also concluded that surface coatings on the fuel cladding can greatly improve radiative heat transfer. Qin et al.[11] conducted an optimization analysis of the energy conversion efficiency and radiator mass of an air-cooled space nuclear reactor and investigated the performance of HPR (heat pipe radiator) and LPR (liquid droplet radiator), respectively. Meng et al.[12] performed numerical simulations of a 1/12 full-core air-cooled space nuclear reactor using the STAR- CCM + program and a series of calculations of a complex core structure under zero-gravity conditions. Li et al.[13] proposed a conceptual design for an integrated space air-cooled reactor based on TRISO fuel with an electrical power output of 200 kW. It was finally concluded that helium-xenon mixture is the optimal work mass. Alfonso Biondi et al.[14] modeled and simulated a closed Brayton cycle system driven by a solar parabolic collector, which improved the efficiency by 7.4%, reduced the weight by 21%, and achieved a specific mass of the system of 30 kg/kW. Guilherme B. Ribeiro et al.[15] developed a closed regenerative Brayton cycle model which is used to calculate the size of the heat exchangers in the system. And the mass of the heat exchangers in the space reactor is also optimized. Wu et al.[16] examined the transient response safety of gas-cooled reactors and investigated the performance of the overall system of coupled Brayton cycles using a self-developed thermal-hydraulic system analysis program. Ma et al.[17]investigated the characteristics of a SNPS with a dual Brayton loop after a single or dual Brayton loop load loss.

He-Xe gas mixtures are often used in reactors on land, sea, air and space. Thanks to the support from the fields of chemistry and gas dynamics, there are many studies on the nuclear aspects of He-Xe gases.Wang et al.[18] optimized a model for the calculation of the physical properties of He-Xe gas mixtures, and obtained a systematic property analysis procedure suitable for the calculation of the natural circulation of He-Xe gas mixtures. Adil Malik et al.[19] analyzed the advantages of using helium-xenon over pure helium in the turbocompressor of a high-temperature gas-cooled reactor (HTGR) power plant. Ma et al.[20]established a link between the thermodynamic performance of a megawatt-scale space reactor system and its mass, and investigated the effects of different binary mixtures of noble gases on the performance and mass of the system. It was finally concluded that helium-xenon mixture is the optimal mass.Wang et al.[21]numerically investigated the thermo-hydrodynamic properties of the He-Xe gas mixture inside a 2×2 helix wrapped rod bundle, which provides a basis for the thermo-hydrodynamic design of He-Xe gas-cooled space nuclear reactors.

The combination of high-temperature gas-cooled reactors (HTGR) and Brayton cycle systems is an important research object for space reactor power supply[22, 23]. Most of the current studies mainly focus on two aspects: the core design of high-temperature gas-cooled reactors and the design optimization of the components in the Brayton cycle, but there are fewer studies on the structural selection of the Brayton cycle. For common gases such as air and supercritical CO2, the structure of different Brayton cycles will have a large impact on the cycle efficiency. As for the He-Xe gas mixture with large adiabatic index, the optimal Brayton cycle structure and the optimal cycle parameters will be sought in this paper on the basis.

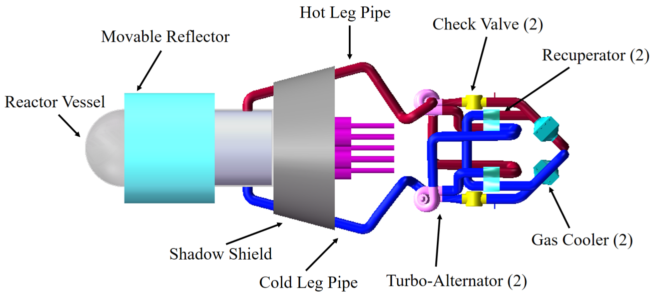

Fig. 1. The cross-section of the gas-cooled reactor coupled Brayton cycle system

II. INTRODUCTION TO THE SYSTEM AND MODEL

A. High Temperature Gas-Cooled Reactor (HTGR) Model

1. High Temperature Gas-Cooled Reactor (HTGR) Model

The high-temperature gas-cooled reactor used in this paper is an open-grid high-temperature gas-cooled reactor[24] , which mainly consists of upper and lower grids, 654 fuel elements and 13 control rods. The upper and lower grids are used for axial positioning of the fuel elements, and the cylindrical fuel elements are arranged in a triangular shape in the core with a spacing of 14.2 mm. The control rods have a B4C core block inside and a 1-mm-thick shell outside, with a gap in the middle made of metal rubber to compensate for the radial deformation caused by fission gases, etc. A schematic diagram of a high-temperature gas-cooled reactor coupled to a Brayton cycle is shown in Fig 1.

The fuel element consists mainly of the uranium dioxide fuel pellet, the hot-end and cold-end reflector layers, the casing and the liner. The core block is a sintered disc of uranium dioxide fuel with an internal center hole, the cladding is made of Mo-Nb-Zr alloy. The center hole serves to vent the gaseous fission products into the gas replenishment space of the fuel element with the help of a dedicated venting device. Table 1 lists the design parameters of the open-grid HTGR:

B. Brayton Cycle Model

The Brayton cycle is a reliable thermal cycle, it has been widely used in many fields by virtue of its efficiency and

Parameter	Value	Parameter	Value
Neutron energy spectrum	fast reactor	Thickness of radial reflective layer/cm	10.3
Reactor power/MWt	3.4	Number of fuel rods	732
Coolant flow/$kg \cdot s^{-1}$	14.236	Number of control rods	13
Control rod conduit outer diameter/cm	3.5	Fuel rod spacing/cm	1.41
Core diameter/cm	41.6	UO_2 Fuel core block inner diameter/mm	3.0
Inner diameter of descending section/cm	44.4	UO_2 Fuel core block outer diameter/mm	10.9
Outer diameter of descending section/cm	46.4	Air gap thickness/mm	0.05
Pressure vessel thickness/cm	0.6	Shell thickness/mm	1.0
Pressure vessel outer diameter/cm	47.6	Fuel area height/cm	55.0

Table 1. Design parameters for open-grid HTGR

applicability[25]. A simple Brayton cycle consists of four main processes: Adiabatic compression, isobaric heating, adiabatic expansion and isobaric exotherm. The core of the Brayton cycle is the TAC, which consists of a turbine, compressor and generator arranged on the same rotor shaft. The work of the turbine is distributed to the compressor and generator through the rotor shaft, allowing the Brayton cycle to operate. In addition to this, there are coolers, recuperators and other components in the space reactor.

The temperature-entropy diagram of a simple reheat Brayton cycle is shown in Fig. 2. First, the high-temperature He-Xe gas mixture from the gas-cooled reactor outlet enters the turbine to do work (1-2). At this point, the high-temperature He-Xe gas mixture enters the recuperator and transfers heat to the other side of the recuperator (2-3). It then enters the external cooler where it is cooled by NaK on the tube side (3-4). The cooler fluid enters the compressor (4-5) and the excess work is used to generate electricity. The fluid then enters the recuperator to be heated by the fluid on the other side (5-6) and finally flows back into the core to be heated to the required turbine inlet temperature (6-1).

In order to maximize the heat utilization, a recompressor is added to the recompression cycle while splitting the recuperator into two. The temperature-entropy diagram of the recompression cycle is shown in Fig 3. Unlike the simple reheat Brayton cycle, the fluid flowing from the low-temperature recuperator is split in two through a splitter, and then enters the main compressor and the recompressor (4-5-6 and 4-7). The fluid passing through the recompressor meets another portion of the fluid heated by the high-temperature recuperator (7-8), and it is finally heated by the low-temperature recuperator and core. This configuration increases the enthalpy at the core inlet, thereby increasing the cycle efficiency for some fluid.

The compressor is the main power-consuming component in the Brayton cycle, and reducing its power consumption can improve the efficiency of the system cycle. The power consumption is related to the compressor inlet temperature. The interstage-cooled cycle divides the compressor into two, and a cooler is added between two compressors, so that the inlet temperature of the second compressor can be reduced. Thus the total power consumption is reduced. The diagram of the interstage cooling cycle is shown in Fig.4.

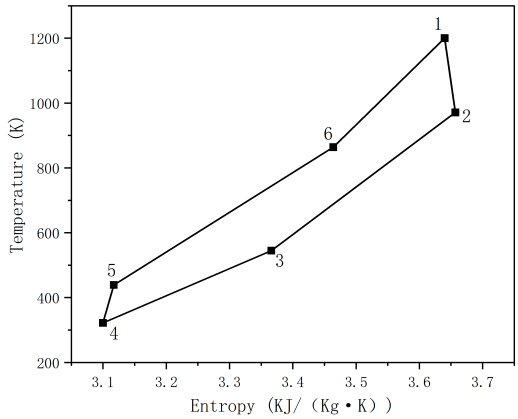

Fig. 2. Temperature-entropy diagram for simple reheat Brayton cycle

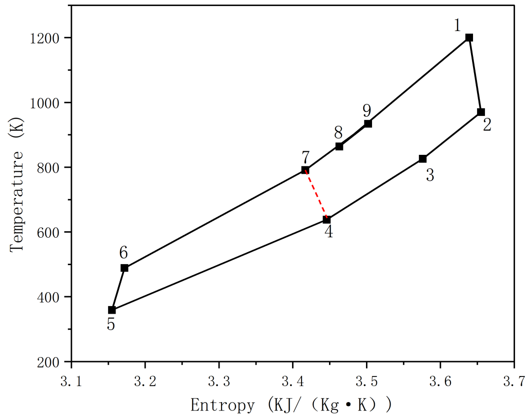

Fig. 3. Temperature-entropy diagram for recompression cycle

C. Turbomachinery model

1) Power balance

The power of the TAC shaft is equal to the power produced by the turbine minus the power consumed by the compressor and generator. This TAC model combines the rotor shaft power with the rotational speed. When the rotor shaft power is positive, the faster the rotor shaft will rotate, and the slower the rotor shaft will rotate when the shaft power is negative. The mathematical expression is given as:

$$\frac{dN_{Shaft}}{dt} = \frac{P_{Shaft}}{I \cdot N_{Shaft} \cdot 4\pi^2} \tag{1}$$

Power balance equation on the rotating shaft:

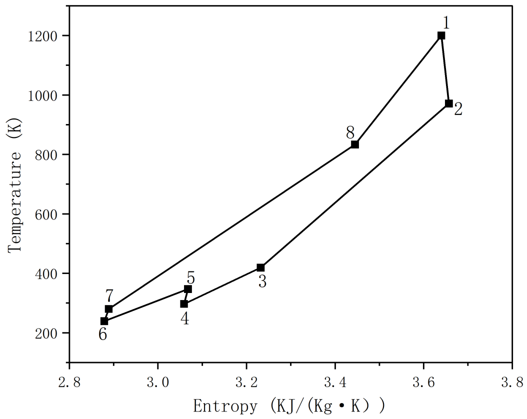

Fig. 4. Temperature-entropy diagram for interstage-cooled cycle

$$P_{Shaft} = P_{Tur} - P_{Com} - P_{Alt} \tag{2}$$

Power generated by the turbine:

$$P_{Tur} = W_{Tur} \cdot C_{p,g}(T_{cin} - T_{cout}) \tag{3}$$

Power consumed by the compressor:

$$P_{Com} = W_{Com} \cdot C_{p,g}(T_{cin} - T_{cout}) \tag{4}$$

Where:N_{Shaft}–TAC rotating shaft speed/s^{-1};P_{Shaft}–TAC rotor shaft power/W; I–Rotor shaft moment of inertia/$kg \cdot s^2$.P_{Tur}–Turbine power/W;P_{Com}–Compressor power;P_{Alt}–AC Generator power/W;T_{tin}–Turbine inlet temperature/K;T_{tout}–Turbine outlet temperature/K;T_{cin}–Compressor inlet temperature/K;T_{cout}–Compressor outlet temperature/K.

2)Flow Characteristic Curve

The work of the turbine and compressor is related to the flow mass flow rate, inlet and outlet temperatures, which can be obtained from the characteristic curve[26]. The flow characteristic curve takes the temperature ratio and pressure ratio as a function of inlet temperature, inlet pressure, mass flow rate and shaft speed, which can be calculated given certain boundary conditions.

Pressure ratio curve of a compressor:

$$\frac{P_{cout}}{P_{cin}} = f_{PrC}(T_{cin}, P_{cin}, W_{Com}, N_{Shaft}) \tag{5}$$

Temperature-ratio curves for pressurized gas engines:

$$\frac{T_{cout}}{T_{cin}} = f_{TrC}(T_{cin}, P_{cin}, W_{Com}, N_{Shaft}) \tag{6}$$

Pressure ratio curve of the turbine:

$$\frac{P_{tout}}{P_{tin}} = f_{PrT}(T_{tin}, P_{tin}, W_{Com}, N_{Shaft}) \tag{7}$$

Temperature-ratio curve of the turbine:

$$\frac{T_{tout}}{T_{tin}} = f_{TrT}(T_{tin}, P_{tin}, W_{Com}, N_{Shaft}) \tag{8}$$

Where:P_{cout}–Compressor outlet pressure/Pa;P_{cin}–Compressor inlet pressure/Pa; f_{PrC}–Equation of the pressure-ratio characteristic curve of the compressor; f_{TrC}–Equation for the compressor temperature-ratio characteristic curve;P_{tout}–Turbine outlet pressure/Pa;P_{tin}–Turbine inlet pressure/Pa;f_{PrT}–Turbine pressure-ratio characteristic curve equation;f_{TrT}–Turbine temperature ratio characteristic curve equation.

D. Heat transfer model

There is at least one gas cooled in every space reactor Brayton cycle, also known as an external cooler. It is an external cold source to cool the Brayton cycle flow mass. It is a shell-and-tube countercurrent heat exchanger with fins, where the high-temperature He-Xe gas is on the shell side and water or liquid NaK flows on the tube side as the cooling medium. The heat absorbed on the tube side is transferred to the space through radiant heat dissipation, thus realizing a continuous discharge of waste heat. Inside the cooler, there are 400 heat exchanger tubes with an outer diameter of 6.35mm, a tube length of 2m, and a wall thickness of 1.058 mm. Including the fins, the effective gas-side heat exchanger area is 47 m^2 . The gas cooler model includes the heat exchanger model for the flow of the fluids on the high and low temperature sides, and the heat conductivity model for the heat exchanger tubes.

The model of the gas cooler includes the flow heat transfer model of the fluid on both sides of the high and low temperatures and the heat conduction model of the heat transfer tube. The two-side flow heat transfer model calculates the pressure and enthalpy of the fluid, and the wall heat conduction model calculates the temperature of the heat exchanger tube, ignoring the axial heat conduction of the heat exchanger tube wall and assuming that the heat is transferred only in the radial direction. The control volume of the model is divided as shown in the Fig 5. First, the high and low temperature side and the heat exchanger tube are divided into N control volumes, and then the heat exchanger tube is divided into N control volumes in the radial direction. Since the heat exchanger is a counter-flow heat exchanger, it should be noted that the numbering order of the high temperature side and the low temperature side should be reversed.

Energy conservation equation for the ith control volume of the gas on the high temperature side:

$$\rho^i_{GC1} c^i_{p,GC1} \frac{dT^i_{GC1}}{dt} \tag{9}$$

$$= \frac{W_{GC1in}(h^{i-1}_{GC1} - h^i_{GC1}) + l_i \prod^i_{GC1} \cdot H^i_{GC1}(T^{M+2,i}_{wall} - T^i_{GC1})}{l_i A_{GC1}} \tag{10}$$

Energy conservation equations for the ith control volume

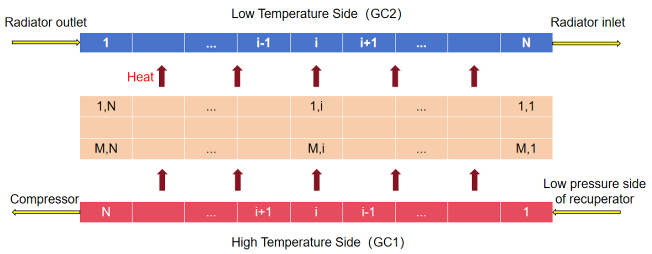

Fig. 5. Schematic diagram of the control volume division of the heat exchanger model

of the cooled mass on the low-temperature side:

$$\rho^i_{GC2}c^i_{p,GC2}\frac{dT^i_{GC2}}{dt} \tag{11}$$

$$= [W_{GC2in}(h^{i-1}_{GC1} - h^i_{GC1}) + N_{pipe}l_iC_{tubeI}H^i_{GC2} \tag{12}$$

$$(T^{1,N-i+3}_{wall} - T^i_{GC2})]/[N_{pipe}\cdot l_iA_{GC2}] \tag{13}$$

Thermal conductivity equation for the (j,i)th control volume of the intermediate heat exchanger wall:

$$N_{pipe}\cdot\rho^{j,i}_w c^{j,i}_{p,w}\frac{dT^{j,i}_w}{A^{j,i}_w} \tag{14}$$

$$= \frac{\prod^{j,i}_{wI}}{A^{j,i}_w}(\frac{\lambda^{j-1,i}_w + \lambda^{j,i}_w}{2})(\frac{T^{j-1,i}_w - T^{j,i}_w}{r^j_w - r^{j-1}_w}) \tag{15}$$

$$+ \frac{\prod^{j,i}_{wO}}{A^{j,i}_w}(\frac{\lambda^{j+1,i}_w + \lambda^{j,i}_w}{2})(\frac{T^{j+1,i}_w - T^{j,i}_w}{r^{m+1}_w - r^m_w}) \tag{16}$$

Boundary conditions on the inner surface of the heat exchanger tube:

$$(\frac{\lambda^{1,i}_w + \lambda^{2,i}_w}{2})\frac{T^{2,i}_w - T^{1,i}_w}{r^2_w - r^1_w} = H^i_{GC2}(T^{1,i}_w - T^{N-i+3}_{GC2}) \tag{17}$$

Boundary conditions on the outer surface of the heat exchanger:

$$(\frac{\lambda^{M+2,i}_w + \lambda^{M+1,i}_w}{2})\frac{T^{M+2,i}_w - T^{M+1,i}_w}{r^{M+2}_w - r^{M+1}_w} = H^i_{GC1}(T^i_{GC1} - T^{M+2,i}_w) \tag{18}$$

Where: $\prod$–Channel heating perimeter/m; H–Convective heat transfer coefficient of the mass/$W\cdot m^{-2}\cdot K^{-1}$;$T_w$–Heat exchanger tube wall temperature/K;W_{in}–Inlet mass flow rate/$kg\cdot s^{-1}$;N_{pipe}–Number of heat exchanger tubes;C_{tubeI}–Heat exchanger tube inner circumference/m;W_{wallI}–Heat exchanger tube control volume inner surface circumference/m;W_{wallO}–Heat exchanger tube control volume outer surface circumference/m; Superscript i–Axial control volume number; Superscript j–Radial control volume number of the heat exchanger tube wall; Subscript GC1–High temperature side; Subscript GC2–Low temperature side; Subscript w–Heat exchanger tube wall.

In addition, in order to improve the utilization of heat and the thermal efficiency of the system, there is at least one plate-fin type recuperator in each Brayton cycle loop. The high-temperature fluid from the turbine outlet transfers the heat to the compressor outlet fluid at the later stage of the cycle, thus realizing the preheating of the work mass. It can increase the enthalpy value of the point to a certain extent and reduce the heat absorbed by the work mass from the heap, so as to make a large improvement in the thermal efficiency of the cycle. The basic model of the recuperator and the gas cooler is the same, and the difference between the two lies in the difference between the high and low temperature side of the work mass.

E. Auxiliary model

He-Xe gas mixtures have an important place in the field of space reactor research, and the combination of a Brayton cycle with a high-temperature gas-cooled reactor using He-Xe gas mixtures as the work mass is well suited for space reactor missions in the MW power missions. For the Brayton cycle circuit, the gas modeling is particularly important. In addition to this, the pressure loss and thermophysical properties of the mass in the pipeline have a significant impact on key parameters such as cycle efficiency.

For the transport properties of He and Xe single gases can be calculated by Chapman-Enskog theory[27], and then the properties of the two can be mixed by the method proposed by Hirschfeld[28], which leads to the properties of He-Xe gas mixture. Since the molecular mass of bothM_w, mole fraction x and adiabatic index γ are known, the average molecular mass of the gas mixture $M_{w0}$and the average adiabatic index γ_0 respectively:

$$M_{w0} = x_{Xe} + (1 - x_{Xe})M_{He} \tag{19}$$

$$\gamma_0 = x_{Xe}\gamma_{Xe} + (1 - x_{Xe})\gamma_{He} \tag{20}$$

The gas constant of the gas mixture is:

$$R_0 = R_g/M_{w0} \tag{21}$$

Where: R_0=8.3145 J/(mol K) is the ideal gas constant. Thus, the density ρ, speed of sound c and specific constant pressure heat capacity of the gas mixture c_p can be calculated by the following equation:

$$\rho(T,p) = p/R_0T \tag{22}$$

$$c(T) = (\gamma R_0T)^{1/2} \tag{23}$$

$$c_p(\gamma, M_w) = R_0/M_{w0}(1 - 1/\gamma) \tag{24}$$

For the calculation of the kinetic viscosity μ and thermal conductivity λ, the Lennard-Jones potential theory is used in Hirschfeld's method, and the Lennard-Jones coefficients for He and Xe are, respectively:

$$\epsilon_{He} = 10.2K, \sigma_{He} = 2.576 \tag{25}$$

$$\epsilon_{Xe} = 229K, \sigma_{Xe} = 4.055 \tag{26}$$

The above coefficients combined with the transport theory prediction curve $\Omega(T)$ The equations for the calculation of the kinetic viscosity μ and thermal conductivity λ of monatomic gases can be obtained.

$$\Omega(T) = 0.92495 + 2.07368 \times 10^{-3} T + 0.719288 T^{-1.151049} - 5.46452 \times 10^{-2} T^{1/2} \tag{27}$$

$$\mu(M_w, \epsilon, \sigma, T) = (M_w T)^{1/2} / \sigma^2 \Omega(T/\epsilon) \times 2.6693 \times 10^{-6} \tag{28}$$

$$\lambda(M_w, \epsilon, \sigma, T) = 8.322 \times 10^{-2} W/m \cdot (T/M_w)^{1/2} / \sigma^2 \Omega(T/\epsilon) \tag{29}$$

The transportation characteristics of the gas mixture can be determined by the following equation:

$$\Phi_{HX}(T) = \frac{1}{\sqrt{8}}(1 + \frac{M_{wHe}}{M_{wXe}})^{-0.5} \cdot [1 + (\frac{\mu_{He}(T)}{\mu_{Xe}(T)})^{0.5} (\frac{M_{wXe}}{M_{wHe}})^{0.25}]^2 \tag{30}$$

$$\Phi_{HX}(T) = \frac{1}{\sqrt{8}}(1 + \frac{M_{wXe}}{M_{wHe}})^{-0.5} \cdot [1 + (\frac{\mu_{Xe}(T)}{\mu_{He}(T)})^{0.5} (\frac{M_{wHe}}{M_{wXe}})^{0.25}]^2 \tag{31}$$

$$\lambda_{mix}(T) = \frac{x_{He}\lambda_{He}(T)}{x_{He} + x_{Xe}\Phi_{HX}(T)} + \frac{x_{Xe}\lambda_{Xe}(T)}{x_{Xe} + x_{He}\Phi_{XH}(T)} \tag{32}$$

$$\mu_{mix}(T) = \frac{x_{He}\mu_{He}(T)}{x_{He} + x_{Xe}\Phi_{HX}(T)} + \frac{x_{Xe}\mu_{Xe}(T)}{x_{Xe} + x_{He}\Phi_{XH}(T)} \tag{33}$$

F. Model verification

EBSILON is a power plant general visualization grouping thermodynamic mechanism modeling and heat balance calculation simulation software. And up to now, the modeling of the S^4 reactor as well as the thermo-hydraulic analysis has been more mature[29]. The reactor is modeled using EBSILON to verify the reliability of EBSILON for the simulation of space reactor, and the relevant parameters of the reactor are referenced in the literature[30]. The simulation results are shown in Table 2:

Parameter	EBSILON calculated value	Literature design value	Aberration	Modelica Language Calculated Values	Aberration
Reactor flow $/kg \cdot s^{-1}$	1.360	1.345	1.115%	1.317	3.265%
Core inlet temperature/K	1144.0	1144.0	0%	1144.44	0%
Turbine outlet temperature/K	970.976	960	1.143%	960	0.23%
Outlet temperature of the hot end of the recuperator/K	556.137	557.6	0.262%	557.6	0.262%
compressor inlet temperature/K	403.0	403.0	0%	/	/
compressor outlet temperature/K	524.812	528	0.604%	/	/
Pile inlet temperature/K	939.651	938.5	0.123%	944.172	0.479%
System power generation/MW	0.0298	0.0301	0.997%	/	/

Table 2. Comparison of simulated and reference values

Compared to the reference values in the literature, the computational aberrations simulated by EBSILON are within the allowable deviation range. So they are therefore sufficient to demonstrate the reliable status of EBSILON in the simulation of space reactor power supply simulations for subsequent analysis.

III. RESULT AND DISCUSSION

A. Comparison of direct and indirect Brayton cycle efficiencies

The direct Brayton cycle and the indirect Brayton cycle have their own advantages and disadvantages in research applications. The direct Brayton cycle is compact and less expensive, but the radioactivity will fill the entire Brayton cycle loop. The indirect Brayton cycle is able to physically separate the primary and secondary loops, thus isolating the radioactivity, but it takes up too much space and has additional power consumption. The direct and indirect Brayton cycle circuits with 40g/mol of helium-xenon gas mixture as the flow medium are simulated by EBSILON with the same thermal power of 3MW. The main pump of the first circuit of the indirect Brayton cycle is replaced by a compressor, and the numerical transmitter is used to control the same flow rate of the first and second circuits. The simulation results are shown in Fig 6: At this time, three parameters, namely turbine inlet temperature, pressure ratio and compressor inlet temperature, were varied to observe the change of the efficiency of the direct and indirect Brayton cycles at different parameters. The results are shown in Fig 7: The results show that the direct and indirect Brayton cycles follow the same trend as each system parameter changes. However, the efficiency of the direct Brayton cycle is 1.4% to 2.8% higher than that of the indirect Brayton cycle. This is because, on the one hand, the system components of the indirect Brayton cycle are more than those of the direct Brayton cycle, which leads to an increase in the pressure loss of the system. On the other hand, the first circuit of the indirect Brayton cycle contains one more pump, which acts as a power-consuming component. So the power dissipation of the system increases, which leads to a decrease in efficiency. Therefore, in practical applications for high-power missions such as deep space exploration, the direct Brayton cycle is more suitable. It has higher efficiency in a more compact structure[31]. Although the indirect Brayton cycle is able to isolate radioactivity in the reactor primary loop, such an advantage is not obvious in

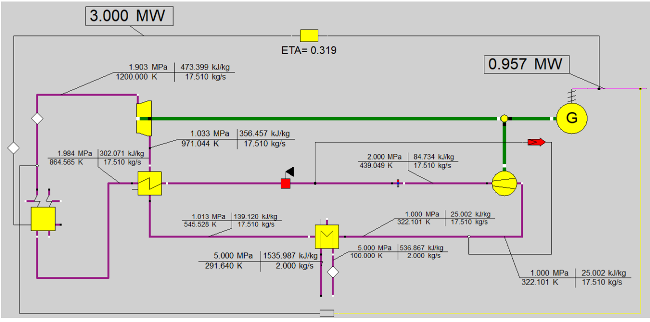

(a)

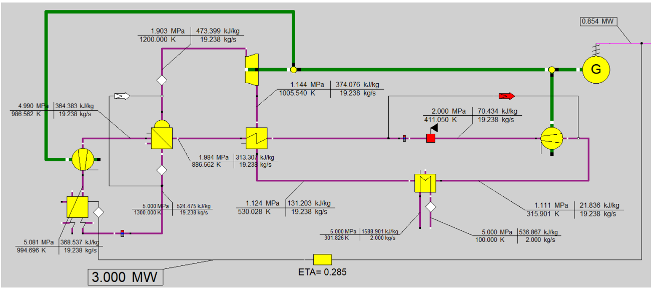

(b)

Fig. 6. The simulation of direct and indirect Brayton cycle in EBSILON

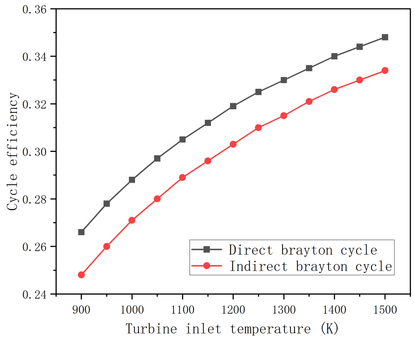

(a)

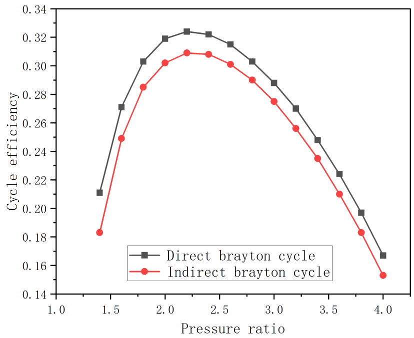

(b)

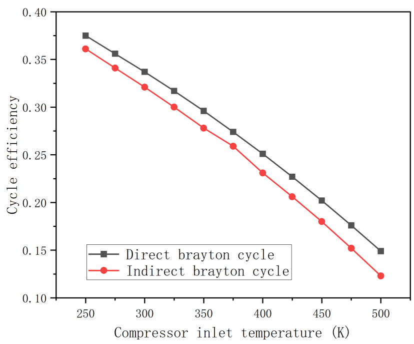

(c)

Fig. 7. The cycle efficiency comparison of the direct and indirect Brayton cycle

specific contexts.

B. Comparison of the efficiency of four Brayton cycle structures

For the Brayton cycle, in order to increase its efficiency, researchers improve its structure by adding interstage-cooled and recompression, among other things. For gases such as air and supercritical CO2, recompression cycle is generally used[32–34]. For helium-xenon gas mixtures which has high adiabatic index, the applicability of different Brayton cycle structures may be different from other types of gases. The four Brayton cycle structures are modeled and simulated using EBSILON, as shown in Fig 8: In EBSILON, both the compressor inlet temperature and the turbine inlet temperature can be used as boundary conditions to design the complete circuit. Therefore, the effect of turbine inlet temperature on the efficiency of different Brayton structures is investigated. And then the efficiency of different Brayton cycle structures is observed and compared. The compressor inlet temperatures are selected of 300K, 350K and 400K, and the turbine inlet temperature varies from 950K to 1500K. The simulation results are shown in Fig 9: As shown in Fig 9 (a), $\eta_{interstage-cooled} > \eta_{simplereheat} > \eta_{interstage-cooledrecompression} > \eta_{recompression}$ at compressor inlet temperature of 400K. When the turbine inlet temperature is 1000K, the recompression cycle efficiency is only 9.1%. And when the turbine inlet temperature is lower than 1200K, the recompression cycle efficiency is lower than 20%. It is due to the large adiabatic index of the helium-xenon mixture (stable at high temperatures around 1.67), which makes the effect of compressor power dissipation larger. When the turbine inlet temperature is higher than 1400K, the efficiency of both interstage-cooled cycle and simple reheat cycle is higher than 30%. The difference in efficiency between the two is less than 2%. Considering the compactness of the structure, the simple reheat cycle is a better structure.

As shown in Fig 9 (b), when the turbine inlet temperature is 1200K and 1500K, the simple reheat cy-

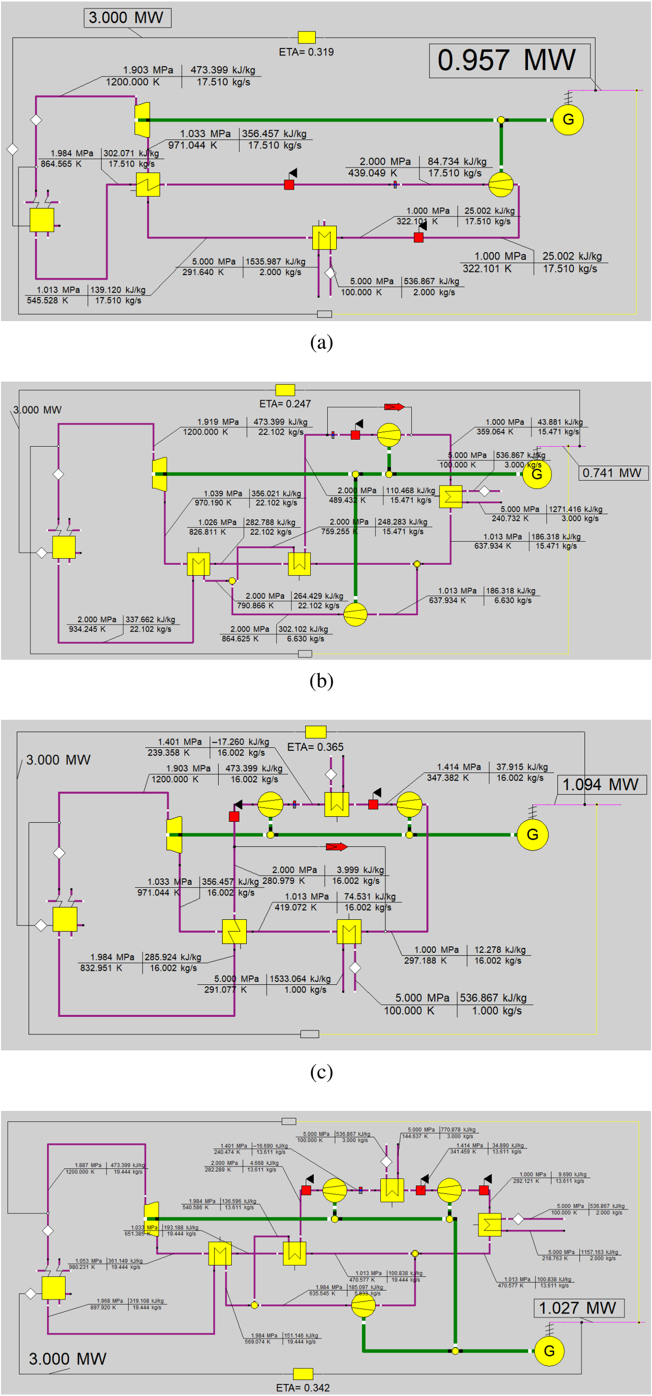

(a)

(b)

(c)

(d)

Fig. 8. The simulation of four structures of Brayton cycle using EBSILON

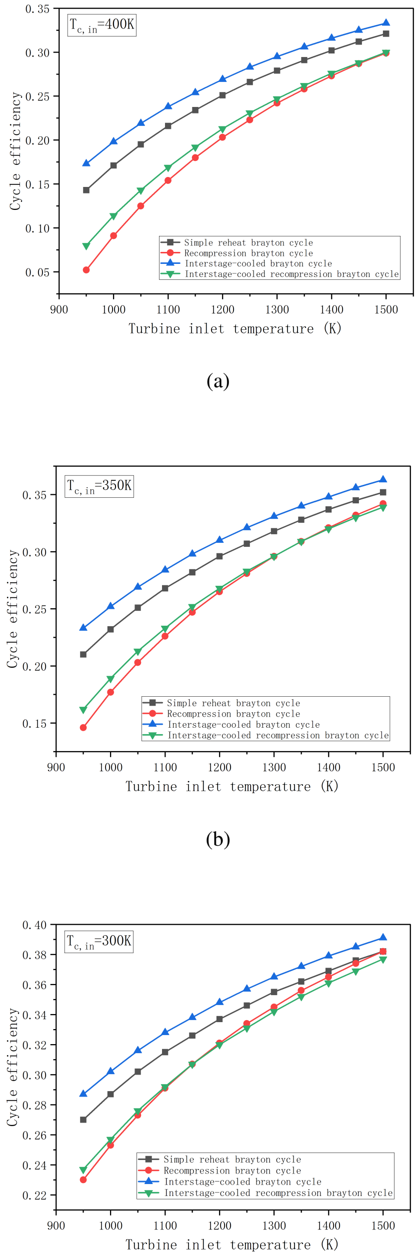

(a)

(b)

(c)

Fig. 9. The simulation results of different Brayton cycle structures

cle efficiency is 29.6% and 35.2%, respectively. And when the turbine inlet temperature is less than 1350K, $\eta_{interstage-cooledrecompression} > \eta_{recompression}$. When the turbine inlet temperature is more than 1350K, $\eta_{interstage-cooledrecompression} < \eta_{recompression}$.

As shown in Fig 9 (c), when the compressor inlet temperature is 300K, the efficiency of all four cycle structures is higher than 20%. And when the turbine inlet temperature is higher than 1150K, the efficiency of all four structures is higher than 30%. Besides, the efficiency of both the recompression cycle and the simple reheat cycle is 38.2% when the turbine inlet temperature reaches 1500K. This is due to the fact that at low compressor inlet temperatures, the additional power dissipation due to the recompressor is low, and the negative effect on the cycle efficiency is close to the positive effect due to the reactor inlet enthalpy increase.

In the actual study, considering the physical properties of

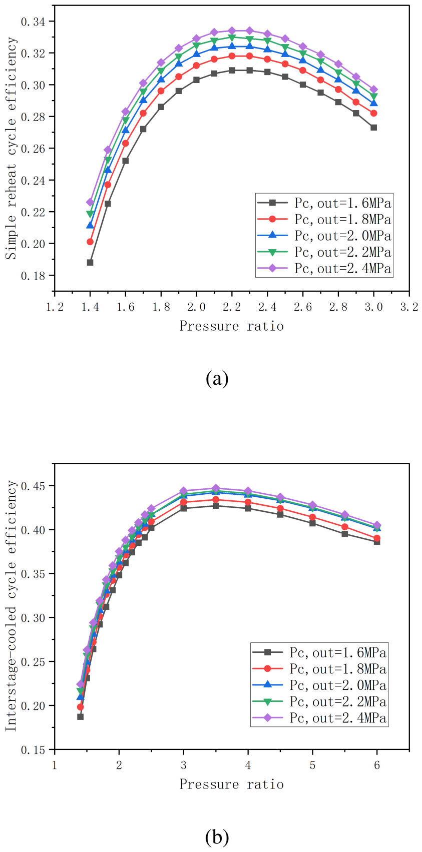

Fig. 10. The effect of the pressure ratio on the Brayton cycle efficiency

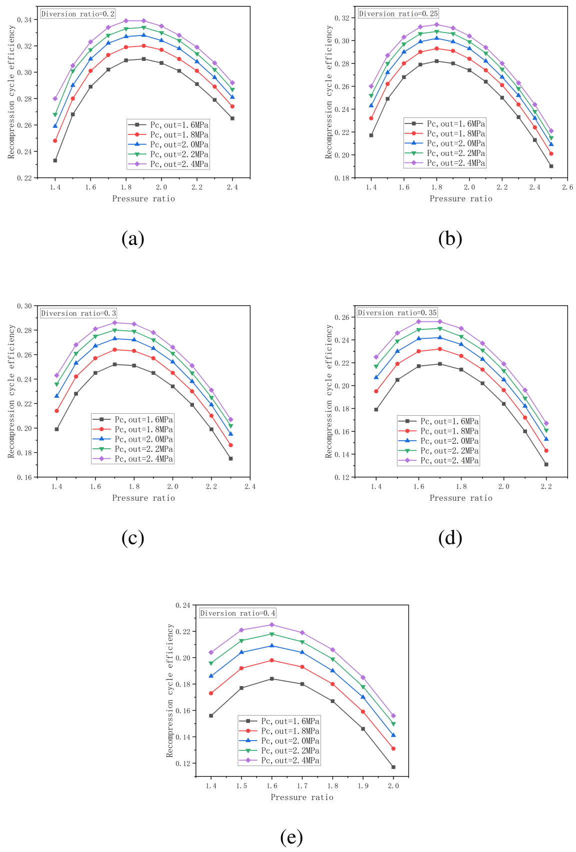

Fig. 11. The effect of the pressure ratio on the recompression Brayton cycle efficiency with different diversion ratios

the work material, the material properties of the components and the cost, it is difficult to further increase the turbine inlet temperature and further reduce the compressor inlet temperature. Therefore, summarizing the above results, The simple reheat cycle has a large advantage regardless of changes in compressor and turbine inlet temperatures.

C. Effect of pressure ratio on efficiency

In the Brayton cycle loop, the maximum and minimum pressure are located at the inlet and outlet of the compressor, and the ratio of the two is called the pressure ratio. In this study, by controlling the compressor outlet pressure to a constant value (1.6MPa, 1.8MPa, 2.0MPa, 2.2MPa, 2.2MPa), the pressure ratio is changed to investigate the effect on the efficiency. The simulation results of simple reheat cycle and interstage-cooled cycle are shown in Fig 10:

For the simple reheat cycle, when the compressor outlet pressure is different, the curves of the cycle efficiency satisfy the trend of increasing and then decreasing, and all of them get the maximum value at the pressure ratio of 2.2. At a pressure ratio of 2.2, the cycle efficiency increases from 30.9% to 33.4% as the compressor outlet pressure increases from 1.6MPa to 2.4MPa. As for the interstage-cooled cycle, the efficiency is more sensitive to the change of pressure ratio before the efficiency obtains the maximum value. And after the efficiency obtains the maximum value, the efficiency changes with the pressure ratio more slowly. Regardless of the value of the compressor outlet pressure, the pressure ratio at which the system's circulation efficiency is maximized is 3.5. And the cycle efficiency increased from 42.7% to 44.7% as the compressor outlet pressure increased from 1.6 MPa to 2.4 MPa.

In addition, the simulation studies on the optimum pressure ratio of the recompression cycle are carried out with the diversion ratios of 0.2, 0.25, 0.3, 0.35, and 0.4, respectively, and the results are shown in Fig 11. The results show that the optimal pressure ratios of the recompression cycles are different at different diversion ratios. The larger the diversion ratio, the smaller the corresponding optimal pressure ratio. The recompression cycle with the optimal pressure ratio achieves the maximum cycle efficiency when the split ratio is 0.2 and the compressor outlet pressure is 2.4 MPa. At this time, the cycle efficiency is 0.339, which is approximately equal to the maximum efficiency of the simple reheat cycle and much smaller than the maximum efficiency of the interstage-cooled cycle.

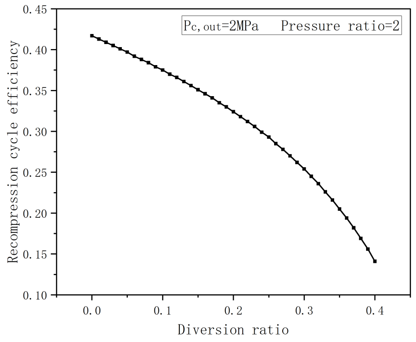

Fig. 12. The effect of the diversion ratio on the recompression Brayton cycle efficiency

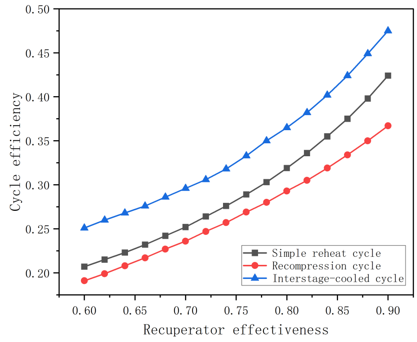

Fig. 13. The influence of the recuperator effectiveness on the cycle efficiency

D. Effect of diverter ratio on recompression efficiency

The above results show that the diversion ratio has an effect on the recompression cycle efficiency. Therefore, the diversion ratio of the splitter is changed to observe the change of the cycle efficiency.. Since the results described in the previous section show that the recompression cycle efficiency has reached a very low level when the pressure ratio is taken as 2.0 and the shunt ratio is 0.4. Therefore, the diversion ratio is changed from 0 to 0.4 to obtain the results shown in Fig 12: When the diversion ratio increases from 0 to 0.4, the efficiency of the recompression cycle decreases, and the magnitude of change is large. Obviously, when the recompression diversion ratio is close to 0, the recompressor does not consume power, and the recompression cycle is infinitely close to the simple recuperation cycle with two recuperators. According to the results of the previous study, the simple reheat cycle efficiency is higher than the recompression cycle, and contains two recuperators, so the cycle efficiency can be increased to 41.7%. And when the diversion ratio tends to 1, the system tends to Brayton cycle without recuperators, the cycle efficiency is greatly reduced. When the diversion ratio is 0.4, the cycle efficiency is only 14.1%.

E. Influence of recuperator on efficiency

On the basis of the above simulation results, the influence of the recuperator effectiveness on the efficiency of Brayton cycle is investigated, and the results are shown in Fig 13: It is easy to find that, regardless of the structure of the Brayton cycle, increasing the recuperator effectiveness can effectively improve the cycle efficiency of the system. When the recuperator effectiveness is increased from 0.6 to 0.9, the simple reheat cycle efficiency is increased by 21.7%. Moreover, when the recuperator effectiveness reaches 0.78, the efficiency of simple reheat cycle can be higher than 30%. For the interstage-cooled cycle, its efficiency is always about 5% higher than that of the simple reheat cycle. However, the simple reheat cycle has greater applicability to the interstage-cooled cycle because it has one more cooler than interstage-cooled cycle.

F. Effect of pressure loss on efficiency

In the Brayton cycle circuit, pressure loss is inevitable, including pressure loss of the cooler, recuperators and other components, as well as the pressure loss of the pipeline. The pipeline pressure loss was divided into high pressure loss and low pressure loss, and the high pressure and low pressure loss were defined in EBSILON by setting the pipeline at the inlet and outlet of the compressor, so as to study the effect of the two on the cycle efficiency of the system respectively. The results of the study are shown in Fig 14.

The results showed that when the high pressure relative pressure loss was increased from 0% to 10%,the efficiency of simple reheat cycle and recompression cycle decreased by 9% and 7%, respectively. Whereas, when the relative low pressure loss was increased from 0% to 10%, the efficiency of both decreased by 7.3% and 5.3%, respectively. The effect of the high pressure relative pressure loss on the cycle efficiency is slightly higher than that of the low pressure relative pressure loss, this is because the effect of the high pressure relative loss on the pressure ratio is higher.

G. Impact of TAC on efficiency

The efficiencies of the turbine, compressor and generator all affect the efficiency of the Brayton cycle, and the efficiencies of the turbine and compressor include isentropic and mechanical efficiencies. The change of the cycle efficiency with different mechanical efficiency is studied by setting the isentropic efficiencies of 0.80, 0.82, 0.84, 0.86, 0.88 and 0.90 for the turbine and compressor. And the effect of the generator efficiency on the cycle efficiency is also carried out. The simulation results are shown in Fig 15. It is easy to see that increasing the efficiency always increases the system cycle efficiency, regardless of the component. For the turbine,

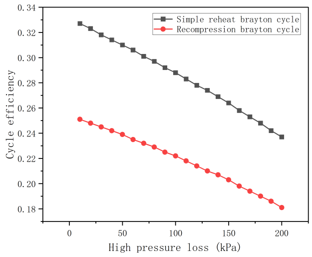

(a)

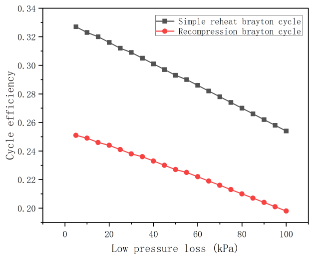

(b)

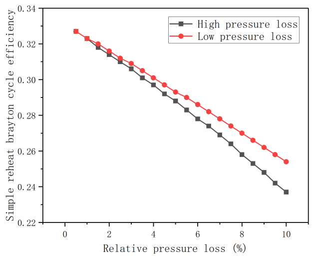

(c)

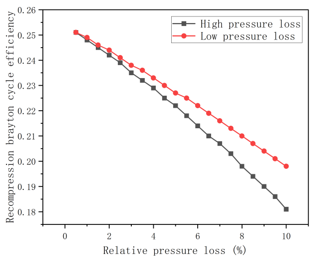

(d)

Fig. 14. The effect of the high and low pressure loss on the cycle efficiency

increasing its mechanical efficiency at a certain isentropic efficiency increases the system cycle efficiency by about 6%. And increasing its isentropic efficiency at a certain mechanical efficiency increases the system efficiency by about 5%. For the compressor, the two values are 3.5% and 5%, respectively. And when the generator efficiency is increased from 0.9 to 0.99, the system efficiency increases by 2.9%.

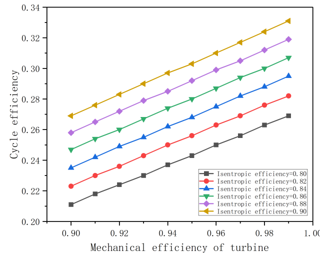

(a)

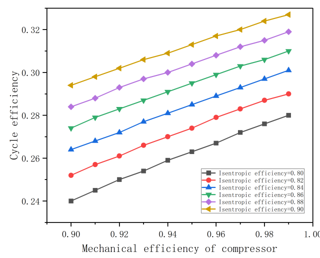

(b)

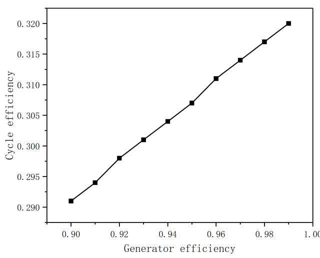

(c)

Fig. 15. The effect of the TAC on the cycle efficiency

H. Exergy analysis

In thermodynamics, exergy is an important parameter. For a cycle loop, analyzing the magnitude and distribution of the energy loss is essential to evaluate its economy and thermal efficiency. Based on the first and second laws of thermodynamics, the method of performance analysis can elucidate the transformations, transfers, utilization, and losses of exergy, and ultimately quantify the performance efficiency of a system or equipment[35].

The method of exergy analysis was used to calculate and analyze the exergy utilization efficiency of Simple reheat cycle and Recompression cycle. And the EBSILON is used to obtain the distribution of the energy loss of the two and to analyze the reasons for the low efficiency of the cycle. And provide guidance for the improvement of their cycle efficiency. The calculated results of the exergy of each component of Simple reheat cycle (1200 K, 2 MPa) are shown in Table 3, Fig. 16 and Fig 17:

		Unit	Turbine inlet	Turbine outlet	Shaft power	
Turbine	Mass flow rate	kg/s	17.510	17.510	/	
	Exergy	kJ/kg	430.593	309.092	2027	
	Exergy loss	kJ/kg	100.483			
	Input	kJ/kg	2127.483			
	Exergy effiency	%	95.277			
Recuperator		Unit	Hot end inlet of the recuperator	Hot end outlet of the recuperator	Cold end inlet of the recuperator	Cold end outlet of the recuperator
	Mass flow rate	kg/s	17.510	17.510	17.510	17.510
	Exergy	kJ/kg	309.092	179.307	184.981	307.332
	Exergy loss	kJ/kg	273.681			
	Input	kJ/kg	2416.047			
	Exergy effiency	%	88.672			
Cooler		Unit	Hot end inlet of the cooler	Hot end outlet of the cooler	Cold end inlet of the cooler	Cold end outlet of the cooler
	Mass flow rate	kg/s	17.510	17.510	2.000	2.000
	Exergy	kJ/kg	179.307	132.529	2289.337	2343.222
	Exergy loss	kJ/kg	583.930			
	Input	kJ/kg	838.636			
	Exergy effiency	%	30.371			
Compressor		Unit	Compressor inlet	Compressor outlet	Comsumed power	
	Mass flow rate	kg/s	17.510	17.510	/	
	Exergy	kJ/kg	132.529	184.981	1056	
	Exergy loss	kJ/kg	89.448			
	Input	kJ/kg	1056			
	Exergy effiency	%	91.530			
Reactor		Unit	Reactor inlet	Reactor outlet	Power input	
	Mass flow rate	kg/s	17.510	17.510	/	
	Exergy	kJ/kg	307.332	430.593	3000	
	Exergy loss	kJ/kg	841.700			
	Input	kJ/kg	3000			
	Exergy effiency	%	71.943			

Table 3. Calculation of the exergy of each part of the Simple reheat cycle

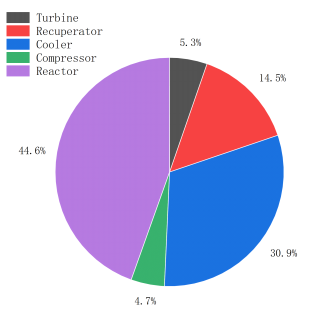

Fig. 16. Proportion of exergy loss in each part of Simple reheat cycle

In Simple reheat cycle, the reactor and external cooler have higher losses, accounting for 44.6% and 30.9% of the total, respectively. The losses in the turbine and compressor are smaller, 5.3% and 4.7%, respectively. The reactor and external cooler also have lower exergy efficiencies, while the latter is only 30.371%, which is one of the major reasons for the lower system efficiency. The calculated results of the densities of the components of the recompression cycle (1200 K, 2 MPa) are shown in Table 4, Fig 18 and Fig 19: As in Simple reheat cycle, the losses in the recompression cycle are concentrated in the reactor and external cooler, which have losses of 37.6% and 42.0%, respectively. The remaining components have relatively small losses. The external cooler of the reactor has a lower energy efficiency, while the energy

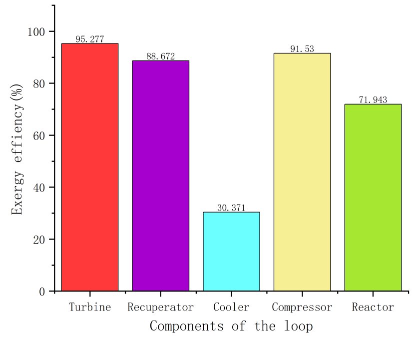

Fig. 17. Exergy efficiency of the main equipment of simple reheat cycle

		Unit	Turbine inlet	Turbine outlet	Shaft power	
Turbine	Mass flow rate	kg/s	22.102	22.102	/	
	Exergy	kJ/kg	431.061	309.102	2568	
	Exergy loss	kJ/kg	127.538			
	Input	kJ/kg	2695.538			
	Exergy effiency	%	95.269			
Recuperator1		Unit	Hot end inlet of the recuperator	Hot end outlet of the recuperator	Cold end inlet of the recuperator	Cold end outlet of the recuperator
	Mass flow rate	kg/s	22.102	22.102	22.102	22.102
	Exergy	kJ/kg	309.102	257.478	282.569	332.557
	Exergy loss	kJ/kg	36.159			
	Input	kJ/kg	1140.994			
	Exergy effiency	%	96.831			
Recuperator2		Unit	Hot end inlet of the recuperator	Hot end outlet of the recuperator	Cold end inlet of the recuperator	Cold end outlet of the recuperator
	Mass flow rate	kg/s	22.102	22.102	15.471	15.471
	Exergy	kJ/kg	257.478	207.511	195.558	272.114
	Exergy loss	kJ/kg	163.846			
	Input	kJ/kg	1348.244			
	Exergy effiency	%	87.847			
Cooler		Unit	Hot end inlet of the cooler	Hot end outlet of the cooler	Cold end inlet of the cooler	Cold end outlet of the cooler
	Mass flow rate	kg/s	15.471	15.471	2.000	2.000
	Exergy	kJ/kg	207.511	137.780	2289.337	2384.808
	Exergy loss	kJ/kg	919.594			
	Input	kJ/kg	1110.536			
	Exergy effiency	%	17.194			
Compressor		Unit	Compressor inlet	Compressor outlet	Comsumed power	
	Mass flow rate	kg/s	15.471	15.471	/	
	Exergy	kJ/kg	137.780	195.558	1041	
	Exergy loss	kJ/kg	80.963			
	Input	kJ/kg	1041			
	Exergy effiency	%	92.223			
Recompressor		Unit	Recompressor inlet	Recompressor outlet	Comsumed power	
	Mass flow rate	kg/s	6.630	6.630	/	
	Exergy	kJ/kg	207.511	307.802	775	
	Exergy loss	kJ/kg	36.915			
	Input	kJ/kg	775			
	Exergy effiency	%	95.237			
Reactor		Unit	Reactor inlet	Reactor outlet	Power input	
	Mass flow rate	kg/s	22.102	22.102	/	
	Exergy	kJ/kg	332.557	431.061	3000	
	Exergy loss	kJ/kg	822.865			
	Input	kJ/kg	3000			
	Exergy effiency	%	72.571			

Table 4. Calculation of the exergy of each part of Recompression cycle

efficiency of the external cooler is only 17.194%, which is the direct reason for the lower recompression efficiency.

Based on the above study, it can be seen that the efficiency

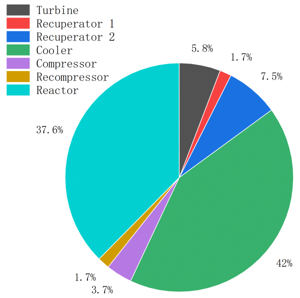

Fig. 18. Proportion of exergy loss in each part of Recompression cycle

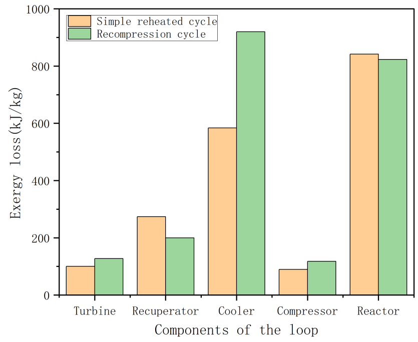

Fig. 20. The exergy loss comparison of Simple reheat cycle and Recompression cycle

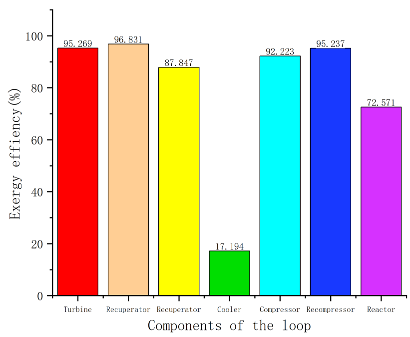

Fig. 19. Exergy efficiency of the main equipment of simple reheated cycle

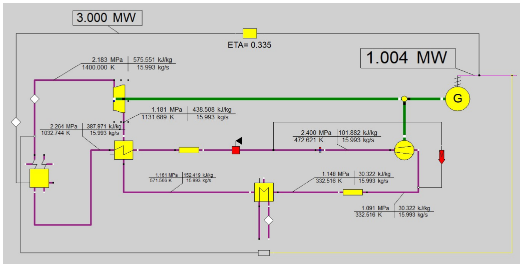

Fig. 21. The system designed in EBSILON

Parameter	Value	Parameter	Value
Thermal power/MWt	3	cyclic efficiency	0.335
Electric power/MWt	1.004	Recuperator effectiveness	0.85
Coolant flow/$kg \cdot s^{-1}$	15.993	Turbomachinery efficiency	0.99
Turbine inlet temperature/K	1400	Turbine isentropic efficiency	0.88
Inlet temperature of the hot end of the recuperator/K	1131.689	Mechanical efficiency of pressurized air	0.99
Cooler inlet temperature/K	571.566	Isentropic efficiency of a pressurized gas engine	0.88
Compressor inlet temperature/K	332.516	Generator efficiency	0.99
Cold end inlet temperature of recuperator/K	472.621	Maximum cycle pressure/MPa	2.4
Pile inlet temperature/K	1032.744	pressure ratio	2.2

Table 5. The parameters of the system designed

of the recompression cycle is lower than that of simple reheat cycle in most cases. By means of the method of exergy analysis, a comparative plot of the energy loss between the two was obtained, as shown in Fig 20: With the exception of the recuperator and the reactor, the recompression cycle has higher losses than the simple reheat cycle. Especially for the external cooler, the loss of the recompression cycle is 919.594 kJ/kg, which is much larger than that of the simple reheat cycle, which is 583.93 kJ/kg.Although the recompression cycle increases the inlet enthalpy of the reactor, the irreversible loss carried away by the external cooler source is much more. And it leads to the reduction of the net system work, and therefore results in the reduction of the system efficiency.

In summary, a simple reheat cycle loop with 3 MW of thermal power and 1 MW of electrical power is designed using EBSILON. The parameters of the system are shown in the Table 4. The system is able to fulfill the space exploration missions at the MW power level and maintains a high loop efficiency while considering a relative pressure loss of 5%. The system schematic is shown in Fig 21.

IV. CONCLUSION

In this paper, the Brayton cycle of a gas-cooled reactor with a thermal power of 3 MW is taken as a research object to study the efficiency comparison of Brayton cycles with different structures as well as the sensitivity analysis, and the main conclusions are as follows:

(1) For the direct and indirect Brayton cycle loops, the efficiency comparison between the two is carried out by vary-

ing the inlet temperatures and pressure ratios of the turbine and the compressor and the rest of the boundary conditions is controlled to be the same. It was found that direct cycle is 1.4% to 2.8% more efficient than indirect cycle.

(2) For four common Brayton cycle configurations, the efficiencies of the four configurations were compared by varying the turbine inlet temperature while controlling for a certain compressor inlet temperature. It is shown that at higher compressor inlet temperatures, recompression cycle negatively affects the efficiency, while the interstage-cooled Brayton cycle and simple reheat cycle have the highest efficiency. The efficiency of both is higher than 30% at turbine inlet temperatures above 1400K.At slightly higher compressor inlet temperatures, the interstage-cooled and simple reheat cycles still have high efficiencies, and when the turbine inlet temperature is less than 1350K, $\eta_{interstage-cooledrecompression} > \eta_{recompression}$, when the turbine inlet temperature is higher than 1350K,$\eta_{interstage-cooledrecompression} < \eta_{recompression}$. At lower compressor inlet temperatures, the efficiency of all four cycles is higher than 20%. At a turbine inlet temperature of 1500K, the efficiency of both the recompression cycle and the simple reheat cycle is 38.2%. The negative effect from the recompressor disappears.

(3) The pressure ratio also has a large effect on the efficiency of the Brayton cycle. For the simple reheat cycle and the interstage cooling cycle, the optimal pressure ratios are 2.2 and 3.5, respectively, and the magnitude of the optimal pressure ratio is independent of the maximum system pressure. For the recompression cycle that needs to consider the split ratio, it is shown that different split ratios correspond to different optimal pressure ratios, and the larger the split ratio is, the smaller the corresponding optimal pressure ratio is;

(4) The diversion ratio has a large effect on the efficiency of the recompression cycle, which decreases as the diversion ratio increases. When the diversion ratio increases from 0 to 0.4, the circulation efficiency decreases from 0.417 to 0.141. This is due to the fact that a low diversion ratio converges to a simple reheat cycle with two recuperators, while a high diversion ratio converges to a Brayton cycle without recuperators. In addition, the number of recuperators and the regenerator effectiveness also have an effect on the efficiency of the Brayton cycle;

(5) By setting the relative pressure loss between the inlet and outlet of the compressor to simulate the pressure loss in the actual working condition, it is found that the high pressure loss has a slightly larger effect. The efficiency of simple reheat cycle and recompression cycle are reduced by 9% and 7% respectively when the high pressure relative loss increases from 0% to 10%.

(6) The efficiency of the TAC components will affect the cycle efficiency to some extent and can be maximized in practical engineering.

[1] H.P. Mei, D.L. Yu, S.Q. Ma et al. Conceptual design for a 5 kWe space nuclear reactor power system[J].NUCLEAR ENGINEERING AND TECHNOLOGY,2024,56,(9):3644-3653.

[2] P. Liu, J. Tian, P. Sun et al. Cascade control system design for a space nuclear reactor[J].ANN NUCL ENERGY,2024,208110760-110760. DOI:10.1016/J.ANUCENE.2024.110760.

[3] Simone D, Bruno C, Czysz A P. Investigation of nuclear electric powered interstellar precursor missions[J].Acta Astronautica,2010,68(7):1193-1200. DOI:10.1016/j.actaastro.2010.10.013.

[4] Koroteev AS, Akimov VN, Popov SA. Project of creation of transport-power module on the basis of nuclear power propulsion system of megawatt type[J]. Poliot Mag, 2011, 4: 93-99.

[5] Blott R, Koppel C, Valentian D, et al. Disruptive Technologies for Power and Propulsion (DiPoP) Fission Nuclear Options[C]. 64th International Astronautical Congress. 2013.

[6] JANSEN F, BAUER W, MASSON F, et al. DEMOCRITOS Demonstrators for Realization of Nuclear Electric Propulsion of the European Roadmaps MEGAHIT&DiPoP[J].T JPN SOC AERONAUT S, AEROSPACE TECHNOLOGY JAPAN, 2016,14(ists30):Pb_225-Pb_233. DOI:10.2322/TASTJ.14.PB_225.

[7] W.X. Ju, K.W. Ning, F.L. Zhao et al. Modelling Research and Performance Analysis on a Megawatt-Level Helium-Xenon Gas Cooled Small Reactor Based on the Thermal-Hydraulic Constraints[J].SSRN,2024,DOI:10.2139/ssrn.4885295.

[8] X. Yang, D. She, L. Shi. Neutronics Analysis of Small Compact Prismatic Nuclear Reactors for Space Crafts[J].JOURNAL OF NUCLEAR ENGINEERING AND RADIATION SCIENCE,2018,4,(2):021006.DOI:10.1115/1.4038774.

[9] B.H. Jiang, Y. Ji , J. Sun et al. Shielding mass estimation model for gas-cooled space nuclear reactors[J].NUCL ENG DES,2024,424,DOI:10.1016/j.nucengdes.2024.113238.

[10] K. Yue, C.L. Wang, R. Zhang et al. Shutdown safety analysis of megawatt-class space gas-cooled reactor system[J].PROG NUCL ENERG,2023,161,DOI:10.1016/j.pnucene.2023.104727.

[11] H. Qin, C.L. Wang, W.X. Tian et al. Energy allocation optimization of the gas-cooled space nuclear reactor[J].APPL THERM ENG,2021,196,DOI:10.1016/j.applthermaleng.2021.117289.

[12] T. Meng, K. Cheng, F. Zhao et al. Computational flow and heat transfer design and analysis for 1/12 gas-cooled space nuclear reactor[J].ANN NUCL ENERGY,2020,135106986-106986.DOI:10.1016/j.anucene.2019.106986.

[13] Z. Li, J. Sun, M. Liu et al. Design of a hundred-kilowatt level integrated gas-cooled space nuclear reactor for deep space application[J].NUCL ENG DES,2020,361(prepublish):110569-110569. DOI:10.1016/j.nucengdes.2020.110569.

[14] Biondi, Alfonso,Toro, Claudia. Closed Brayton Cycles for Power Generation in Space:Modeling,simulation and exergy analysis[J].ENERGY,2019,181, 793-802.

[15] Ribeiro Guilherme B, Braz Filho Francisco A, Guimaraes Lamartine N. F. Thermodynamic analysis and optimization of a Closed Regenerative Brayton Cycle for nuclear space power systems[J].APPLIED THERMAL ENGINEERING,2015,90,250-257.

[16] Y. Wu, S. Tang, L. Zhu, et al.Transient analysis of megawatt-level space gas-cooled reactor coupled with He-Xe Brayton cycle system[J].APPL THERM ENG,2025,260124962-

124962.DOI:10.1016/J.APPLTHERMALENG.2024.124962

[17] W.K. Ma, P. Ye, Y. Gao, et al. Study on the load loss characteristics of a space nuclear power system with multi Brayton loops[J].ANN NUCL ENERGY,2023,185. DOI:10.1016/J.ANUCENE.2023.109702.

[18] Xianbo W, Xianmin D, Zhongchun L, et al. Transient characteristics analysis of residual heat removal system for Helium-Xenon mixture cooled small reactor system[J].NUCL ENG DES,2023,410.DOI:10.1016/J.NUCENGDES.2023.112387.

[19] Malik A, Zheng Q, Lin A. The design and performance analysis of highly loaded compressor of closed Brayton cycle HTGR power plant with helium xenon gas mixture as working fluid[J].Progress in Nuclear Energy,2019,117103084-103084. DOI:10.1016/j.pnucene.2019.103084.

[20] W.K. Ma, P. Ye, G. Zhao et al. Effect of cooling schemes on performance of MW-class space nuclear closed Brayton cycle[J].ANN NUCL ENERGY2021,162,DOI:10.1016/j.anucene.2021.108485.

[21] C.L. Wang, S.Y. C, W.X. Tian et al. Thermal-hydraulic analysis of He–Xe gas mixture in 2×2 rod bundle wrapped with helical wires[J].NUCL ENG TECHNOL,2023,55(7):2534-2546.DOI:10.1016/J.NET.2023.04.013.

[22] King JC, El-Genk MS. Thermal-hydraulic and neutronic analyses of the submersion-subcritical, safe space (S^4) reactor[J]. NUCL ENG DES, 2009, 239(12): 2809-2819.

[23] B. Jiang, Y. Ji, J. Sun et al. Dynamic analysis code development for space nuclear power systems[J].PROG NUCL ENERG,2025,180105601-105601. DOI:10.1016/J.PNUCENE.2024.105601.

[24] Koroteev AS, Akimov VN, Popov SA. Project of creation of transport-power module on the basis of nuclear power propulsion system of megawatt type[J]. Poliot Mag, 2011, 4: 93-99.

[25] H. Liao, F. Zhao, H. Bao, et al.Preliminary analysis of startup and acceleration transient characteristics of helium-xenon cooled reactor direct brayton cycle system[J].PROG NUCL ENERG,2024,177105462-105462. DOI:10.1016/J.PNUCENE.2024.105462.

[26] Wright SA, Lipinski RJ, Vernon ME, et al. Closed Brayton cycle power conversion systems for nuclear reactors: modeling, operations, and validation[J]. Sandia Rep, 2006: 1-257.

[27] T. M B, M. B. Diffusion coefficient of krypton atoms in helium gas at low and moderate temperatures[J].MOL PHYS,2007,105(1):51-58. DOI:10.1080/00268970601129050.

[28] HIRSCHFELDER J O, CURTISS C F,BIRDR. Molecular theory of gases and fluids[M].New York:John Wiley and Sons,1954.

[29] King C J, El-Genk S M. Submersion-Subcritical Safe Space (S 4) reactor[J].NUCL ENG DES,2005,236(17):1759-1777. DOI:10.1016/j.nucengdes.2005.12.010.

[30] A. Zhang, X. Wang. Development of Modelica-based one-dimensional thermodynamic cycle library and its application in simulation and multi-objective optimization of a He-Xe closed-Brayton-cycle system[J].PROG NUCL ENERG,2024,172,DOI:10.1016/j.pnucene.2024.105205.

[31] W. Ma, X. Yang, J. Wang. Power regulation methods and regulation characteristics of the space reactor direct Brayton cycle with helium-xenon working fluid[J].Energy,2024,313134012-134012. DOI:10.1016/J.ENERGY.2024.134012.

[32] G.Y. Peng, Y.C. Peng, Z. Na, et al. Multi-objective optimization and evaluation of supercritical CO2 Brayton cycle for nuclear power generation[J].NUCL SCI TECH,2024,35(2).DOI:10.1007/S41365-024-01363-Y.

[33] Ahn Y, Lee J, Kim G S, et al. Design consideration of supercritical CO 2 power cycle integral experiment loop[J].Energy,2015,86115-127. DOI:10.1016/j.energy.2015.03.066

[34] Park H J, Park S H, Kwon G J, et al. Optimization and thermodynamic analysis of supercritical CO2 Brayton recompression cycle for various small modular reactors[J].Energy,2018,160520-535. DOI:10.1016/j.energy.2018.06.155.

[35] H. Hu, Y. Jiang, C. Guo, et al. Thermodynamic and exergy analysis of a S-CO2 Brayton cycle with various of cooling modes[J].ENERG CONVERS MANAGE,2020,220. DOI:10.1016/j.enconman.2020.113110.